Reversible Morphological Control of Tubulin-Encapsulating Giant Liposomes by Hydrostatic Pressure

*Masahito Hayashi, † Masayoshi Nishiyama, ‡, §, * Yuki Kazayama, ∥ Taro Toyota, ∥, ⊥ Yoshie Harada, ‡ and Kingo Takiguchi, †, ¶, **

† Division of Biological Science, Graduate School of Science, Nagoya University, Nagoya 464-8602, Japan. ‡ Institute for Integrated Cell–Material Sciences (WPI–iCeMS), and § The HAKUBI Center for Advanced Research, Kyoto University, Kyoto 606-8501, Japan. ∥ Graduate School of Arts and Sciences, and ⊥ Research Center for Complex Systems Biology, The University of Tokyo, 3-8-1 Komaba, Meguro-ku, Tokyo 153-8902, Japan. ¶ Structural Biology Research Center, Nagoya University, Nagoya 464-8601, Japan.

KEYWORDS

Artificial cell model, Microtubule (MT), Cell-sized giant liposome, Control of membrane vesicle morphology, Hydrostatic pressure.

ABSTRACT

To develop an artificial cell-like chemical-machinery, liposomes encapsulating cytoskeletons have drawn much recent attention. However, as far as we know, there has been no report showing isothermally reversible morphological changes of liposomes containing cytoskeletons because the sets of various regulatory factors, *i.e.*, their interacting proteins, are required to control the state of every reaction system of cytoskeletons. Here we focused on hydrostatic pressure to control the polymerization state of microtubules (MTs) within cell-sized giant liposomes (diameters ~ 10 μm). MT is the cytoskeleton formed by the polymerization of tubulin, and cytoskeletal systems consisting of MTs are very dynamic and play many important roles in living cells, such as the morphogenesis of nerve cells and formation of the spindle apparatus during mitosis. Using real-time imaging with a high-pressure microscope, we examined the effects of hydrostatic pressure on the morphology of tubulin-encapsulating giant liposomes. At ambient pressure (0.1 MPa), many liposomes formed protrusions due to tubulin polymerization within them. When high pressure (60 MPa) was applied, the protrusions shrank within several tens of seconds. This process was repeatedly inducible (around three times), and after the pressure was released, the protrusions regenerated within several minutes. These deformation rates of the liposomes are close to the velocities of migrating or shape-changing living cells rather than the shortening and elongation rates of the single MTs which have been previously measured. These results demonstrate that the elongation and shortening of protrusions of giant liposomes is repeatedly controllable by regulating the polymerization state of MTs within them by applying and releasing hydrostatic pressure.

1. Introduction

To comprehend the superior ability of living cells, constructive approaches such as the reconstitution or construction of cell-like molecular robots that reproduce cell abilities have become significant. Among such approaches, the development of cell-sized giant liposomes encapsulating cytoskeletons has drawn much attention.[1–4] Giant liposomes have closed lipid bilayer membranes and have been used as envelopes for cell-like molecular robots because of their simple structures and capability to be observed directly under optical microscopes.

Cytoskeletons play essential roles in morphogenesis, reinforcement of shape, and deformation and/or movement of living cells and cell organelles. Microtubules (MTs) are one type of cytoskeleton, like actin, intermediate filaments and septin.[5,6] MTs are formed by the polymerization of tubulin (about 100 kDa). Tubulin is a hetero-dimer protein consisting of α– and β–tubulins, which resemble each other; the former is a guanosine triphosphate (GTP)-binding protein and the latter is a guanosine triphosphatase (GTPase). Reversely, MTs can depolymerize to tubulin. MTs are well known as a cytoskeleton that exhibits a dynamic kinetics, can perform a variety of roles by the cooperating with various regulatory systems consisting of MT-associating proteins (MAPs) and/or two different classes of molecular motors, kinesins and dyneins. MTs are very susceptible to physical and chemical stimuli such as changes in temperature, hydrostatic pressure and the addition of reagents.[5–8] When MTs work in various activities of living cells, they exert their functions in two ways: i) by repeating polymerization and depolymerization to elongate and shorten themselves like a stretchable bar, and ii) by interacting with molecular motors to generate sliding forces or movements. The former works primarily for the morphogenesis and movement of cells. The latter is responsible for the

transportation of membrane vesicles and protein complexes inside cells, and for biologically specialized motile apparati, such as muscles and flagella or cilia.

Recently, giant liposomes encapsulating tubulin have been prepared and their morphology and behavior have been reported as follows: Tubulin-encapsulating giant liposomes, the shape of which were spherical before tubulin polymerization, can form protrusions such as those produced by living cells.[9,10] The majority of them maintain a bipolar shape with a central sphere and two tubular protrusions that are aligned in a straight line at room temperature and ambient pressure. To induce morphological changes of giant liposomes, the assembly and elongation of MTs within them was sufficient. However, the liposome deformation could only be induced once for each liposome, and no one has demonstrated further altering their morphology or repeating the deformation. The reasons are that, MTs encapsulated in vesicle are difficult to control from the outside, and naturally the regulation system of MTs consists of the sets of various their interacting proteins, such as MAPs, and/or modification enzymes.

To enable repetition of the deformation of tubulin-encapsulating giant liposomes, we focused on the application and release of hydrostatic pressure on them. Hydrostatic pressure is a major physical parameter that determines the state of every molecular reaction system as does temperature. Compared with changing the temperature, changing the hydrostatic pressure has an advantage in that there is no concern about gradient formation in the specimens. Moreover, the application of hydrostatic pressure of several hundred MPa (1 bar = 0.1 MPa) usually does not seriously affect protein structures, but it does weaken protein-protein and protein-ligand interactions in aqueous solutions.[11–15] The pressure-driven effects are thought to be caused by the enhancement of the clustering of water molecules around hydrophobic and hydrostatic residues on the protein surface. This means that applied pressure enables the modulation of the

polymerization and depolymerization kinetics of cytoskeletons such as MTs, without requiring the use of any chemical reagents or MAPs other than water molecules.[16,17]

In order to visualize the pressure-induced changes in the structure and function of biomacromolecules, we have developed a high-pressure microscope that enables to acquire various microscopic images with high-resolution and sensitivity even when hydrostatic pressure is applied.[18,19] It revealed that applied pressure dynamically changes the motility of molecular motors such as kinesin, F_1–ATPase and bacterial flagellar motors.[17,20,21] Thus, in this study, using the high-pressure microscope, we investigated the pressure-induced morphological changes of tubulin-encapsulating giant liposomes. The results obtained demonstrate that the morphology of tubulin-encapsulating giant liposomes is reversibly and repeatedly controllable by regulating the polymerization and depolymerization of MTs inside the giant liposomes by changing the hydrostatic pressure, which means that MTs are an excellent motion device to develop an artificial motile cell model.

2. Materials and Methods

2.1. Reagents

1,2-Dioleoyl-*sn*-glycero-3-phosphocholine (DOPC), 1,2-dioleoyl-*sn*-glycero-3-phospho-(1'-*rac*- glycerol) (DOPG), cholesterol, liquid paraffin, squalene, chloroform and methanol were purchased from Wako Pure Chemical Industries (Osaka, Japan). 1,2-Distearoyl-sn-glycero-3-phosphoethanolamine-*N*-[methoxy(polyethyleneglycol)-2000] (DSPE-mPEG(2000)) was purchased from Avanti Polar Lipids (Alabaster, AL, USA). Alexa fluor 488, carboxylic acid and succinimidyl ester was purchased from Thermo Fisher Scientific (Waltham, MA, USA). Other chemicals, including GTP, PIPES, EGTA and salts, were of analytical grade and were purchased

from Wako Pure Chemical Industries or Nacalai Tesque (Kyoto, Japan). These chemicals were used without further purification.

2.2. Preparation of Tubulin

Tubulin was prepared from porcine brain by three cycles of polymerization and depolymerization, as described previously.[22] Tubulin solutions were stored at −80°C until used, and GTP was added appropriately.[23] For fluorescence microscopy observations, the purified tubulin was labeled with Alexa fluor 488 in the same way as the fluorescent labeling of actin, and the labeled tubulin was purified by repeating the cycle of polymerization of tubulin and depolymerization of MTs.[22,24]

Since it has been reported that tubulin concentrations in living cells are tens of μM,[25,26] a tubulin solution containing 6.8 mg/mL tubulin (68 μM of tubulin-α and -β hetero-dimer) in BRB80 (80 mM PIPES-HCl (pH 6.8), 1 mM $MgCl_2$ and 1 mM EGTA) containing GTP (200 μM) was used in this study. Before encapsulation into giant liposomes, the tubulin solution was kept on ice for more than 30 min to depolymerize the tubulin.

2.3. Preparation of Tubulin-Encapsulating Giant Liposomes

Giant liposomes were prepared both by the natural swelling method and by a method utilizing a water-in-oil (W/O) emulsion.[9,27,28] For the natural swelling method, DOPC and DOPG (1:1, mol/mol) were dissolved in a chloroform/methanol solution (98:2, vol/vol) at 10 mM as a total lipid concentration. Forty μL of the lipid solution was put into a round-bottom glass test tube. The organic solvent was slowly evaporated under nitrogen flow to form a dry lipid film, which contained 400 pmol lipid molecules. The lipid film was further dried *in vacuo* for more than 90

min. To encapsulate the tubulin dimer into giant liposomes, 20 μL of the tubulin solution was put on the lipid film. The test tube was kept on ice for 30 min to let the lipid film swell. The suspension of tubulin-encapsulating giant liposomes was transferred into another test tube and kept on ice until use (within 2 hr after swelling). In the case where giant liposomes encapsulated no protein for the control experiment, 20 μL BRB80, instead of the tubulin solution, was put on the lipid film.

In the method using W/O emulsion, DOPC, cholesterol and DSPE-mPEG(2000) (10:1:0.2, mol/mol) were dissolved in a mixture of liquid paraffin and squalene (9:1, vol/vol) using a hot stirrer at 65°C under nitrogen gas. The total concentration of lipids was 11.2 mM. To make the W/O emulsion covered with a lipid monolayer, 20 μL of the solution of lipids dissolved in oil and 1 μL of the tubulin solution were mixed in a PCR tube (200 μL, INA OPTIKA, Osaka, Japan) by vigorous tapping. The emulsion was put on top of an aqueous solution, which was consisting in external solution of the liposome, in another PCR tube. The tube was kept on ice for 10 min. The test tube was centrifuged at 18,800 ×G at 4°C for 30 min. The liposomes were precipitated on the bottom of the PCR tube. The oil phase was removed with a micropipette and the pellet was gently suspended and collected with a micropipette. The liposome suspension was transferred into another test tube and kept on ice until observation.

2.4. High-Pressure Microscopy

A high-pressure microscope was constructed to acquire high-resolution microscopic images, regardless of the applied pressure (Figure 1). The pressure apparatus could apply pressure up to 150 MPa. The details of the system were described previously.[18] Briefly, the high-pressure chamber was connected to a separator, a pressure gauge and a high-pressure pump. The separator

conferred the advantage of reducing the total dead volume of the buffer solution in the pressure line. Hydrostatic pressure was applied to the pressure line using a hand pump. The inside of the Teflon cap was filled with buffer solution and was connected to the chamber. The water pressure was transduced to the buffer solution by deformation of a thin Teflon cap in the separator and the pressure was then transmitted to the chamber. We changed the internal pressure by several dozen MPa within a few sec without any overshooting. Pressure was also released nearly instantaneously by opening a valve. The hydrostatic pressure in the pressure line was measured using a pressure gauge.

These pressure devices were combined with an inverted microscope (Ti–E, Nikon, Tokyo, Japan) on a vibration-free table. A metal halide lamp (PhotoFluor II, Burlington, VT, USA) was used as the illumination light source for acquiring phase-contrast images in the chamber. The emission line at 546 nm was collimated and then introduced to the condenser lens. Microscopic observations were carried out using a long-working-distance objective lens (NA=0.6, working distance ~3 mm; CFI ELWD ADM40×C, Nikon). The observations of liposomes were performed at 25°C unless otherwise noted. The phase-contrast images were acquired by a charge-coupled device camera (WAT-120N+ (its successor model is WAT-910HX), Watec, Tsuruoka, Japan). All microscopic images were stored in a computer, and then analyzed offline, using Image J computer software (http://imagej.nih.gov/ij/).

2.5. Temperature Change Experiment on Tubulin-Encapsulating Giant Liposomes

For a reference experiment to investigate morphological changes of tubulin-encapsulating giant liposomes, the suspension of tubulin-encapsulating giant liposomes was enclosed between a slide glass (1 mm thick) and a cover glass (0.17 mm thick) (Matsunami Glass Ind., Kishiwada,

Japan) with a frame-seal incubation chamber (0.3 mm thick) (Bio-Rad, Hercules, CA, USA). Using the sealed chamber, the liposome suspension was not vaporized in the repeated experiment of temperature change. The glass slide was kept on an aluminum block chilled on ice for more than 30 min until microscopic observation. The glass slide was put on an observation stage of a BX60 microscope (Olympus, Tokyo, Japan), which was made of di-cast aluminum, at room temperature to assemble MTs through tubulin polymerization in giant liposomes. To depolymerize MTs in the giant liposomes, the glass slide was transferred to the chilled aluminum block and kept for 30 min. The phase-contrast images were acquired by the charge-coupled device camera (Watec). All microscopic images were stored in a computer, and then analyzed using Image J software as described above.

3. Results

3.1. Reversible Deformation of Tubulin-Encapsulating Giant Liposomes by the Application and Release of Hydrostatic Pressure

We enclosed giant liposomes in the high-pressure chamber, and then tracked the morphology of the same liposome at various pressure conditions (Figure 2). It is noted here that, unless otherwise specified, each observed result shown in this report was obtained by tracking the same liposome. When giant liposomes encapsulated no protein, they were spherical under ambient pressure. Their shape, size and behavior were not affected even when the hydrostatic pressure was increased to 100 MPa (Figures 2a and S1).[29] This result indicates that the pressure-induced deformation of empty giant liposomes could not be achieved, at least under the conditions used in this study.

In the case of tubulin-encapsulating giant liposomes (Figure 2b), MTs assembled and elongated in giant liposomes as the result of the polymerization of tubulin dimers encapsulated under ambient pressure. When their lengths exceeded the diameter of the liposome, they began to push the membrane from within. The liposome deformed from a sphere to an ellipsoid and then to a lemon-like shape, after which it developed protrusions. Finally, the MT-encapsulating giant liposome took a spindle-like shape that consisted of a central spherical part and long protruding tubular parts (the left panel of Figure 2b).

Before the application of pressure, no changes were evident in the morphology of MT-encapsulating giant liposomes, and the protrusion length was constant over time. In contrast, when the pressure was increased from 0.1 to 60 MPa, the protrusions started to shorten from both ends (the second panel from the left of Figure 2b). As the protrusions shortened, the boundary between the central spherical part and the protruding parts became obscure, and some liposomes became indefinite shapes with flabby membranes.

After the release of pressure, the two protrusions reappeared, mostly at the same positions in the liposome, and then elongated with time. The protrusion length finally returned to the initial value before pressure treatment (the center panel of Figure 2b). Unless changing the conditions such as pressure, no changes were evident in the morphology of the liposomes and the protrusion length was constant over time. To make sure of the reversibility of this effect, especially that it could be reproduced many times, we repeated the high-pressure treatment on the same sample liposome dispersion (the first and second panels from the right of Figure 2b). The results showed that the two protrusions of the same liposome shortened at 60 MPa, and then elongated again after the release of pressure (Figure 2c), indicating that this reversible deformation was repeatedly inducible. The difference in results between cases where the giant liposomes did or

did not contain MTs, indicates that the application of pressure directly and reversibly acts on MTs inside the liposomes, resulting in the deformation of the spindle-like shaped liposomes. The basis of the reversibility of the liposome deformations demonstrated here might be the result of summing the changes taking place in lipid membrane and MTs under the high pressure. But still the key factor is the sensitivity of MT against hydrostatic pressure because it is the first achievement that could be realized by the tubulin encapsulation.

3.2. Rate of Liposome Deformation caused by Changing the Hydrostatic Pressure

The pressure-induced changes in the morphology of MT-encapsulating giant liposomes were then studied using time-lapse microscopy. We measured the end-to-end distance between the tips of the membrane protrusions of the same MT-encapsulating giant liposome at specific intervals (Figure 3). When the pressure was increased from 0.1 to 60 MPa at the time of 0 sec, the protrusions started to shorten from both ends. The shortening rate of the long axis length at 60 MPa was 0.92 μm/sec. The pressure-induced shortening of the protrusions reached an equilibrium within about 15 sec after the shortening began. After the release of pressure, two protrusions reappeared, usually at the same positions in the liposome, and then elongated with time. The re-elongation velocity was 2.5×10^{-2} μm/sec at ambient pressure. Therefore, the tubulin-encapsulating giant liposome deformed into a spindle-like shape that shortened quickly at high pressure and then grew again slowly at ambient pressure. It is noted that, in this report, the average rates of a good area of the linearity in the plots are shown.

Next, we compared the shortening rate of the long axis length of spindle-shaped liposomes when varying the applied pressure. Figure 4a displays the time courses of the length changes at 40, 60, and 80 MPa. The length changes were constant over time. The shortening rate depended

on the strength of the applied pressure. As shown in Figure 4b, the logarithm of the shortening rate was proportional linearly to the pressure. This tendency was the same as the relationship previously obtained about single MT.[17] The pressure dependence of the rate, k, was characterized as:

$$k = \alpha \times \exp[-(p - 0.1) \times \Delta V^{\ddagger} / k_{\mathrm{B}}\mathrm{T}], \qquad \text{---------- (1)}$$

where α is the basal rate at 0.1 MPa, p is the pressure, $\Delta V^{\ddagger}$ is the activation volume, and $k_B T$ is the thermal energy. The plots were fitted by Eq. 1 by $\alpha = 8.5 \times 10^{-3}$ μm/sec and $\Delta V^{\ddagger} = -0.23$ nm^3 (−140 mL/mol).

3.3. Reversible Deformation of Tubulin-Encapsulating Giant Liposomes by Changing Temperature

To clarify the effect of hydrostatic pressure on MT polymerization and depolymerization inside the tubulin-encapsulating giant liposomes, we examined the regulation of liposome dynamics by temperature change as a reference experiment. The MT-encapsulating giant liposomes were reversely deformed by placing them at a low temperature (on ice) and then were re-deformed by returning the temperature to 27°C (Figure S2). This reversible de-deformation/re-deformation cycle of liposomes was observed repeatedly by changing the temperature (Figure 5). Namely, the liposomes changed their shape repeatedly between a shape close to a sphere and a spindle-like shape in synchronization with the disassembly and reassembly of MTs inside induced by low (0°C) and high (27°C) temperatures, respectively.

In the case of changing temperature as well as changing hydrostatic pressure, the direction of the long axis of the spindle-shaped liposome was consistent with the orientation of MT polymerization in the liposome (Figure 5). Also, in the case when the temperature was changed,

liposomes that had been deformed into a spindle-like shape de-deformed (*i.e.*, shortened their protrusions) quickly at low temperature and re-deformed (*i.e.*, re-elongated their protrusions) slowly at room temperature (Figure 6). The de-deformation of liposomes observed on ice occurred in the range of several sec to a few min, whereas the re-deformation observed at room temperature took tens of min or several hr.

The re-elongation rate of protrusions observed when the temperature was returned to room temperature ($1 \sim 2 \times 10^{-2}$ μm/sec, Figure 6b) was roughly the same as that observed when the pressure was released to ambient pressure (2.5×10^{-2} μm/sec, Figure 3d), suggesting that the pressure treatment (≤ 90 MPa) did not denature tubulin dimers. The shortening of protrusions induced on ice was estimated as 0.1 ~ 0.2 μm/sec at minimum because all liposomes with long axis lengths of a few tens of μm were de-deformed within 5 min. In a simple comparison, it is a similar rate to those induced by the application of high pressure at more than 60 MPa (Figures 4b and S2).

4. Discussion

4.1. Significance and Application of Tubulin-Encapsulating Giant Liposome

In this study, using the high-pressure microscope, we investigated the pressure-induced morphological changes of tubulin-encapsulating giant liposomes. The results obtained here demonstrate that the morphology of tubulin-encapsulating giant liposomes is reversibly and repeatedly controllable by regulating the polymerization and depolymerization of MTs inside the liposomes by the application and release of hydrostatic pressure, which means that MTs are an excellent motion device to develop an artificial motile cell model. In fact, the shortening rate of a

full length MT at about 40 MPa is in good agreement with the shortening rate of the long axis length of the spindle apparatus during mitosis of living cells.[30]

There are two significant points of the current findings. First, this study successfully shows the potential of cell control by hydrostatic pressure, as well as by temperature, and is the first step in the demonstration of mechanobiology. The results demonstrated here indicate for the first time that changing the pressure is useful to reversibly control the morphology of MTs associated with lipid bilayer deformation in the vicinity of MTs. Second, the results obtained in this study may develop into molecular robotics in order to construct an artificial motile cell model for the basis of regenerative medicine. Of course, this will require a combination of utilizing MT-regulating factors from living cells,[31,32] and/or other methods for manipulating the shape of membrane vesicles.[33–36]

Currently, several methods to deform membrane vesicles have been developed.[2,27,37] In order to construct an artificial motile cell model prospectively, advanced organization of the array of MTs will be necessary. For example, utilizing the nucleus for MT assembly, which will determine the sites of MTs assembly, and/or molecular motors that can slide MTs, that is kinesins or dyneins, should be feasible.[38,39]

In this study, we focused on polymerization and depolymerization of MTs inside liposomes, and the initial condition of the liposomes was spherical shape that is easy to observe morphological changes. The combination with the experiments using liposomes that had been deformed into non-spherical shapes by other proteins or the osmotic pressure is an interesting future work.

4.2. The Reversible Deformation of Tubulin-Encapsulating Giant Liposomes

Most simply, we assume that all encapsulated tubulin dimers exceeding the critical concentration assemble into MTs, and that most MTs have the same length as the end-to-end distance between the two membrane protrusions, since the two protrusions usually form in one straight line, *i.e.*, the long axis direction of the deformed liposome, and a columnar structure was often visible at the region along the long axis in phase contrast and in dark-field images (Figure 2b).[9,10] Regarding the protein and critical concentrations thereof of the encapsulated tubulin solution, the number of MTs involved in the deformation was roughly estimated as several dozens.[40] During the cycle of application and release of hydrostatic pressure, each liposome reached almost the same long axis length when the sample was at ambient pressure (Figure 2c), indicating that the release of tubulin from liposomes in this cycle was negligible.

After several cycles of pressure application, we found that the membrane of some of the tubulin-encapsulating giant liposomes became flabby under the released pressure. Previously, we repeated the cycle of elongation and shortening of the protrusions that had been produced in giant liposomes by manipulating two beads encapsulated within them using optical tweezers.[41–43] As a result, in the second or subsequent cycles, we found that some liposomes began to show an unclear deformation by slackening, which may be due to the discharge of water from the liposomes during the shape changes. The reason for the flabby membranes observed in this study is probably the same. It is noted here that, the previous studies have revealed that the development of a membrane protrusion on a spherical giant liposome require a few tens of pN and the elongation of the protrusion require several pN.[41–43] The force of this range is the strength that dozens of MTs can be enough generating.

When the application and release of pressure was repeated over a long period, the reversible de-deformation/re-deformation cycle of MT-encapsulating liposomes could be repeatedly

induced around three times. This is plausible because the tubulin activity is expected to decrease eventually due to the consumption of GTP and/or the generation of GDP. GTP is indispensable for the functions of MTs because the polymerization and depolymerization process of MTs is closely coupled with the hydrolysis of GTP bound to β–tubulin.[44,45] In addition, it has been found that GDP, the product of GTP hydrolysis, affects the assembly feature of MTs and suppresses their elongation.[23] The deficiency of GTP and the generation of GDP are thought to be the reason that limits the number of times that the liposome deformation can be repeated. Thus, in order to overcome that restriction, a system for maintaining the concentrations of guanine nucleotides, such as a regeneration system of GTP or a channel unique to nucleotides, will be required.[46,47]

4.3. The Shortening of the Membrane Protrusions induced by the Application of Pressure

The shortening rate of full length MTs in a liposome should coincide with the shortening rate of the end-to-end distance between its two membrane protrusions (Figure S3). It should be noted that the two ends of a MT are different from each other.[48] One is the plus end where both elongation and shortening take place much faster, and thus is dynamic, while the other is the minus end where both elongation and shortening take place slower, and thus is stable. In the case where MTs depolymerize only at the plus end when the pressure is increased, the depolymerization rate equals the shortening rate of the end-to-end distance between the membrane protrusions. On the other hand, in the case where MTs depolymerize at both ends equally, as shown in a previous study using paclitaxel-treated MTs,[17] the depolymerization rate at each end of the MT is half of the shortening rate of the end-to-end distance between the membrane protrusions. These two cases are the extremes. Importantly, in either case, the matters discussed in this report are not affected.

The activation volume obtained (–0.23 nm^3 (–140 mL/mol)) was consistent with those of the pressure dependence of the disassembly rate of MTs determined in bulk solution by turbidity measurement (–0.15 nm^3 (–90 mL/mol)),[16] and the shortening rate of single paclitaxel-stabilized MTs observed with a high-pressure microscope (–0.17 nm^3 (–100 mL/mol)).[17] The results show that there was no difference between the characteristics of the pressure dependence of the shortening rate of MTs and the shortening rate of membrane protrusions of the deformed liposomes, regardless of the number of involved MTs, of the stabilization by such reagents as paclitaxel, or of the confinement into a membrane vesicle.[16,17,30] That equivalence suggests that the shortening process under these conditions have a common mechanism. Prospectively, using point mutations of the tubulin dimer,[49] which region(s) of this protein is involved in the polymerization kinetics and the pressure sensitivity will be revealed, and that knowledge will help our understanding of the overall behavior of MTs in living cells. Structural change in tubulin dimer caused under high pressure remains unclear, while studies investigating the effect of pressure on the organism or isolated protein are now in progress.[50,51] Incidentally, the typical example of the natural high-pressure conditions is deep–sea, so that, in relation to the feature of tubulin and MT in the deep-sea organisms, it is an important issue.

On the other hand, the shortening rate of the end-to-end distance between the membrane protrusions of spindle-shaped giant liposomes extrapolated at 0.1 MPa (*i.e.*, the ambient pressure) was 8.5×10^{-3} μm/sec. This is about two orders of magnitude faster than the shortening rate of a single paclitaxel-treated MT extrapolated at 0.1 MPa (6.3×10^{-5} μm/sec), even though the experimental conditions and protein samples are not the same.[17] Actually, the shortening rate of deformed liposomes directly measured at 60 MPa (0.92 μm/sec) was more than three orders of magnitude faster compared with the single paclitaxel-treated MT previously measured at the

same pressure in bulk solution using a high-pressure microscope.[17] In this study, MTs that polymerized in liposomes were not stabilized with paclitaxel. Thus, the stabilization of MTs by paclitaxel, which is indispensable to maintain the polymerized state of MTs even in dilute conditions suitable for microscopic observation, should be a major reason for the large difference between the results. These results suggest that paclitaxel inhibits the depolymerization of MTs but does not affect the characteristics of the pressure-induced depolymerization of MTs. It has been reported that the application of high hydrostatic pressure is able to induce not only depolymerization from the ends, but also breakage at various areas of MTs.[17] However, since the frequency of the breakage was very low, it is not the reason for very fast shortening of the liposome protrusions.

Rather importantly, the extrapolated shortening rate of deformed liposomes (8.5×10^{-3} μm/sec at 0.1 MPa) was slow, one-several tenths of the directly observed shortening rates of an individual MT that was without any modification and this was due to the dynamic instability in bulk solution.[23,30,52–57] Note here that MTs repeat their elongation and shortening states individually even in an equilibrium condition, and this unique nature is called dynamic instability.[30,52–54] As described above, the protruding parts of deformed liposomes should be supported by several dozens of MTs from within. Therefore, in order to shorten the membrane protrusions, all of those MTs have to depolymerize to shorten. The shortening rate of a membrane protrusion plausibly corresponds to the shortening rate of the MT that is depolymerizing with the slowest rate among MTs that exist in the protrusion. Although the shortening rates obtained here reflect the sum of results of many MTs that were encapsulated in the membrane vesicle, these findings are the first results measured under high pressure using MTs that had not been modified.

4.4. The Elongation of the Membrane Protrusions at Ambient Pressure

The re-elongation rate of the end-to-end distance between the protrusions of MT-encapsulating liposomes at ambient pressure (2.5×10^{-2} μm/sec) was approximately one order of magnitude slower than the elongation rate of MTs in bulk solutions that were observed experimentally or expected at similar tubulin dimer concentrations from already known kinetics of MT polymerization.[16,23,52,55–57] The tension in the liposome membrane can be considered as a resistance against deformation and thus is a factor decreasing the elongation rate of the membrane protrusions. In addition, many MTs had to elongate in concert with each other in order to elongate the membrane protrusion, and this effect may also decrease the rate. The elongation rate of protrusions of tubulin-encapsulating giant liposomes at ambient pressure has approximately the same order of magnitude as the velocity of migrating or shape-changing living cells.[58] Of course, cytoplasm of living cells contain many kinds of components other than MT, and so that, is much more complex system in comparing with the tubulin-encapsulating liposomes used in this study. In addition, morphogenesis and movement of a living cell are frequently propelled by molecular motors and regulated by contacts with other cells or extracellular matrix. So that, the mechanism that determines the rate of morphological change is quite different between living cells and the liposomes. As mentioned above, to improve our cell model, especially to be able to regulate freely the rate of morphological changes, we will require a combination of the current cell model with the utilization of other factors such as is present in living cells.

As described above, MTs have polarity because their two ends are different from each other with respect to their elongation and their shortening rates. In the current study, the polarities of

MTs that assembled inside the liposomes remain unknown. The deformed giant liposomes mostly possessed two protrusions. After returning the deformation of spindle-shaped liposomes by the application of pressure, no difference was observed in the re-elongation rate between both protrusions of the same liposome when the pressure was released again to ambient (Figures 2b and 3a–c). This result suggests that the polarities of MTs in the liposomes are random, that is, there are approximately the same numbers of parallel and anti-parallel MTs. Thus, as mentioned above, in order to construct an artificial motile cell model prospectively, providing asymmetry in the array of MTs, *e.g.*, utilizing the nucleus for MT assembly, which will consist of a scaffold of the minus ends of MTs, and/or molecular motors that can slide multiple MTs simultaneously, which will function as a polarity sorter of MTs, will be necessary.[38,39]

5. Conclusions

The effect of hydrostatic pressure on tubulin-encapsulating cell-sized giant liposomes was investigated using a high-pressure microscope. In the cycle of application and release of hydrostatic pressure, many liposomes formed protrusions due to the assembly of MTs within them at ambient pressure and those protrusions shrunk within tens of sec at high pressure. This process was reversible and could be induced repeatedly. We found that the elongation rate of the membrane protrusions of tubulin-encapsulating giant liposomes at ambient pressure had approximately the same order of magnitude as the velocity of migrating or shape-changing living cells, and that both the elongation and shortening rates of the membrane protrusions were not the same as those of MTs previously observed in bulk solutions. This is plausibly because the changes in the morphology of liposomes resulted from the combination of changes that were going on in MTs, which were without any modification (for example, stabilization by paclitaxel),

and assembled in the confined space of the liposome. The findings in this study should help to develop molecular robotics in order to construct an artificial motile cell model driven by hydrostatic pressure cycle.

FIGURE CAPTIONS

Figure 1. High-pressure microscope. **(a)** Schematic diagram of the high-pressure microscope. **(b)** Photograph of the high-pressure microscope.

Figure 2. Reversible deformation of tubulin-encapsulating giant liposomes induced by the application and release of pressure. **(a)** Sequence of phase contrast images showing the morphology of a giant liposome that encapsulated no protein during changes in pressure (control). The liposome was spherical throughout the observation, and did not show any change in shape or size regardless of the pressure (Figure S1). **(b)** Sequence of phase contrast images showing the morphology of a giant liposome that encapsulated tubulin during changes in pressure. It is noted that the two images on the right side were average images of sequential video images within 5 sec in order to correct the defocus. In (a) and (b), the pressure applied is indicated at the bottom of each frame. Scale bars in (a) and (b) indicate 5 and 10 μm, respectively. It is noted here that, unless otherwise specified, each observed result shown in this report was obtained by tracking the morphological change of the same liposome. **(c)** End-to-end distance of the liposome in (b); shortening at 60 MPa occurred within 30 sec, and elongation at 0.1 MPa occurred within about 10 min (see Figure 3).

Figure 3. Reversible shrinkage of protrusions caused by the application and release of pressure. **(a, b,** and **c)** Sequence of phase contrast images of a MT-encapsulated giant liposome. The elapsed time (in sec) after the application of high pressure and the pressure (MPa) that has been applied are indicated at the bottom of each frame. At first, the hydrostatic pressure was 0.1 MPa (a), and the high pressure of 60 MPa was applied at the time of 0 sec (b). Then, at the time of 28 sec, the pressure was returned to 0.1 MPa (c). Scale bar indicates 10 μm. **(d)** Time course of the end-to-end distance between tips of protrusions of the liposome shown in (a – c). Inset shows the result of the whole period. The period when the pressure was 60 MPa is indicated by a gray background; at other periods, the pressure was 0.1 MPa. It should be noted that the shortening rate at 60 MPa was 0.92 μm/sec, and the elongation rate at 0.1 MPa was 2.5×10^{-2} μm/sec. Movies S1 and S2 are short movies made from the sequential images obtained during the shortening process at 60 MPa (b) and re-elongation process at 0.1 MPa (c) of the protrusions of the MT-encapsulating liposome.

Figure 4. Shortening rate of the end-to-end distance between membrane protrusions of a liposome at high pressure. **(a)** Typical examples of the shortening process under various pressures. The cases of 40 (circles), 60 (squares) and 80 (triangles) MPa are shown. The high pressure was applied at the time of 0 sec. The results were obtained from different individual liposomes. **(b)** Semi-logarithmic plot of the shortening rate of the distance between the tips of the protrusions. The points plotted correspond to the results obtained from individual liposomes (n=21). The plots were fitted by Eq. 1 with $\alpha = 8.5 \times 10^{-3}$ μm/sec and $\Delta V^{\ddagger} = -0.23$ nm^3.

Figure 5. Reversible deformation of fluorescent-labeled tubulin-encapsulating liposomes controlled by temperature. Sequences of phase contrast (upper) and fluorescent (lower) images of a tubulin-encapsulated liposome are shown. The elapsed time (min) is indicated below each frame. The observation chamber was cooled on ice for 5 min just before t = 0 and 25 min, and was transferred to the microscope at 27°C. The scale bar indicates 10 μm. Positions of the tips of protrusions are indicated with arrowheads. The ratio of the fluorescence-labeled tubulin is 0.10 (mol/mol).

Figure 6. Reproduction of membrane protrusions of a MT-encapsulating giant liposome at 25°C after treatment on ice. **(a)** Sequence of phase contrast images of the liposome. The elapsed time (min) after the start of the observation is indicated at the bottom of each frame. The bar indicates 10 μm. **(b)** Time course of the end-to-end distance between the membrane protrusions of the liposome shown in (a).

ASSOCIATED CONTENT

Supporting Information

The diameter of a giant liposome that encapsulated no protein when the pressure was changed between 0.1 and 100 MPa. The morphology of MT-encapsulating giant liposomes, which were put on ice and then incubated at 25°C. Model showing the relationship between the de-deformation of a MT-encapsulating liposome and the shortening of a MT encapsulated into the liposome. Two movies showing the reversible deformation of an MT-encapsulating liposome. This information is available free of charge via the Internet at http://pubs.acs.org.

AUTHOR INFORMATION

Corresponding Author

* To whom correspondence should be addressed. Phone: +81-52-788-6248 (K.T.); +81-75-753-9828 (M.N.). FAX: +81-52-747-6471 (K.T.); +81-75-753-9843 (M.N.). E-mail: j46037a@nucc.cc.nagoya-u.ac.jp (K.T.); mnishiyama@icems.kyoto-u.ac.jp (M.N.).

Conflict of Interest

The authors declare no conflict of interest.

ACKNOWLEDGMENTS

This work was supported by a Grant-in-Aid for Scientific Research on Innovative Areas "Molecular Robotics" (Project No. 24104004 to M.H. and K.T., and Project No. 24104005 to

Y.K. and T.T.) and “Harmonized Supramolecular Motility Machinery and Its Diversity” (Project No. 15H01319 to M.N.) and “Thermal Biology” (Project No. 26115708 to Y.H.) of the Ministry of Education, Culture, Sports, Science, and Technology of Japan, and a Grant-in-Aid for Challenging Exploratory Research (Project No. 24651134 to K.T.) of the Japan Society for the Promotion of Science.

ABBREVIATIONS

DOPC, 1,2-Dioleoyl-*sn*-glycero-3-phosphocholine; DOPG, 1,2-dioleoyl-*sn*-glycero-3-phospho-(1'-*rac*- glycerol); DSPE-mPEG(2000), 1,2-distearoyl-sn-glycero-3-phosphoethanolamine-N-[methoxy(polyethylene glycol)-2000]; MT, microtubule; GTP, guanosine triphosphate.

REFERENCES

(1) Yoshikawa, K.; Nomura, S. M.; Tsumoto, K.; Takiguchi, K. Construction of an In Vitro Model of a Living Cellular System. *The Minimal Cell: The Biophysics of Cell Compartment and the Origin of Cell Functionality*, Luisi, P. L., Stano, P., (Eds.) Springer, **2010,** pp. 173–194.

(2) Hagiya, M.; Konagaya, A.; Kobayashi, S.; Saito, H.; Murata, S. Molecular Robots with Sensors and Intelligence. *Acc. Chem. Res.* **2014**, *47,* 1681–1690.

(3) Fujiwara, K.; Yanagisawa, M. Generation of Giant Unilamellar Liposomes Containing Biomacromolecules at Physiological Intracellular Concentrations using Hypertonic Conditions. *ACS Synth. Biol.* **2014,** *3,* 870–874.

(4) Toyota, T.; Banno, T.; Nitta, S.; Takinoue, M.; Nomoto, T.; Natsume, Y.; Matsumura, S.; Fujinami, M. Molecular Building Blocks and their Architecture in Biologically/Environmentally Compatible Soft Matter Chemical Machinery. *J. Oleo Sci.* **2014,** *63,* 1085–1098.

(5) Fischer, R. S.; Fowler, V. M. Thematic minireview series: The State of the Cytoskeleton in 2015. *J. Biol. Chem.* **2015,** *290,* 17133–17136.

(6) Alfaro-Aco, R.; Sabine Petry, S. Building the Microtubule Cytoskeleton Piece by Piece. *J. Biol. Chem.* **2015,** *290,* 17154–17162.

(7) Brouhard, G. J. Dynamic Instability 30 Years Later: Complexities in Microtubule Growth and Catastrophe. *Mol. Biol. Cell* **2015,** *26,* 1207–1210.

(8) Inoué, S.; Salmon, E. D. Force Generation by Microtubule Assembly/Disassembly in Mitosis and Related Movements. *Mol. Biol. Cell* **1995,** *6,* 1619–1640.

(9) Kaneko, T.; Itoh, T. J.; Hotani, H. Morphological Transformation of Liposomes Caused by Assembly of Encapsulated Tubulin and Determination of Shape by Microtubule-Associated Proteins (MAPs). *J. Mol. Biol.* **1998,** *284,* 1671–1681.

(10) Hotani, H.; Miyamoto, H. Dynamic Features of Microtubules as Visualized by Dark-Field Microscopy. *Adv. Biophys.* **1990,** *26,* 135–156.

(11) Mozhaev, V. V.; Heremans, K.; Frank, J.; Masson, P.; Balny, C. High Pressure Effects on Protein Structure and Function. *Proteins* **1996,** *24,* 81–91.

(12) Bartlett, D. H. Pressure Effects on In Vivo Microbial Processes. *Biochim. Biophys. Acta* **2002,** *1595,* 367–381.

(13) Boonyaratanakornkit, B. B.; Park, C. B.; Clark, D. S. Pressure Effects on Intra- and Intermolecular Interactions within Proteins. *Biochim. Biophys. Acta* **2002,** *1595,* 235–249.

(14) Akasaka, K. Highly Fluctuating Protein Structures Revealed by Variable-Pressure Nuclear Magnetic Resonance. *Biochemistry* **2003,** *42,* 10875–10885.

(15) Luong, T. Q.; Kapoor, S.; Winter, R. Pressure-A Gateway to Fundamental Insights into Protein Solvation, Dynamics, and Function. *ChemPhysChem* **2015,** *16,* 3555–3571.

(16) Salmon, E. D. Pressure-Induced Depolymerization of Brain Microtubules In Vitro. *Science* **1975,** *189,* 884–886.

(17) Nishiyama, M.; Kimura, Y.; Nishiyama, Y.; Terazima, M. Pressure-Induced Changes in the Structure and Function of the Kinesin-Microtubule Complex. *Biophys. J.* **2009,** *96,* 1142–1150.

(18) Nishiyama, M.; Sowa, Y. Microscopic Analysis of Bacterial Motility at High Pressure. *Biophys. J.* **2012,** *102,* 1872–1880.

(19) Nishiyama, M. High-Pressure Microscopy for Studying Molecular Motors. *Subcell Biochem.* **2015,** *72,* 593–611.

(20) Okuno, D.; Nishiyama, M.; Noji, H. Single-Molecule Analysis of the Rotation of F_1-ATPase under High Hydrostatic Pressure. *Biophys. J.* **2013,** *105,* 1635–1642.

(21) Nishiyama, M.; Sowa, Y.; Kimura, Y.; Homma, M.; Ishijima, A.; Terazima, M. High Hydrostatic Pressure Induces Counterclockwise to Clockwise Reversals of the Escherichia coli Flagellar Motor. *J. Bacteriol.* **2013,** *195,* 1809–1814.

(22) Karr, T. L.; White, H. D.; Purich, D. L. Characterization of Brain Microtubule Proteins Prepared by Selective Removal of Mitochondrial and Synaptosomal Components. *J. Biol. Chem.* **1979,** *254,* 6107–6111.

(23) Tanaka-Takiguchi, Y.; Itoh, T. J.; Hotani, H. Visualization of the GDP-Dependent Switching in the Growth Polarity of Microtubules. *J. Mol. Biol.* **1998,** *280,* 365–373.

(24) Kouyama, T.; Mihashi, K. Fluorimetry Study of N-(1-Pyrenyl) Iodoacetamide-Labelled F-Actin; Local Structural Change of Actin Protomer Both on Polymerization and on Binding of Heavy Meromyosin. *Eur. J. Biochem.* **1981,** *114,* 33–38.

(25) Hiller, G.; Weber, K. Radioimmunoassay for Tubulin: a Quantitative Comparison of the Tubulin Content of Different Established Tissue Culture Cells and Tissues. *Cell* **1978,** *14,* 795–804.

(26) Goldmacher, V. S.; Audette, C. A.; Guan, Y.; Sidhom, E.-H.; Shah, J. V.; Whiteman, K. R.; Kovtun, Y. V. High-Affinity Accumulation of a Maytansinoid in Cells via Weak Tubulin Interaction. *PLoS One* **2015,** *10,* e0117523.

(27) Takiguchi, K.; Yamada, A.; Negishi, M.; Honda, M.; Tanaka-Takiguchi, Y.; Yoshikawa, K. Construction of Cell-Sized Liposomes Encapsulating Actin and Actin-Cross-Linking Proteins. *Methods Enzymol.* **2009,** *464,* 31–53.

(28) Natsume, Y.; Toyota, T. Giant Vesicles Containing Microspheres with High Volume Fraction Prepared by Water-in-Oil Emulsion Centrifugation. *Chem. Lett.* **2013,** *42,* 295–297.

(29) Nicolini, C.; Celli, A.; Gratton, E.; Winter, R. Pressure Tuning of the Morphology of Heterogeneous Lipid Vesicles: A Two-Photon-Excitation Fluorescence Microscopy Study. *Biophys. J.* **2006,** *91,* 2936–2942.

(30) Salmon, E. D. Pressure-Induced Depolymerization of Spindle Microtubules. *J. Cell Biol.* **1975,** *65,* 603–614.

(31) Olmsted, J. B. Non-Motor Microtubule-Associated Proteins. *Curr. Opin. Cell Biol.* **1991,** *3,* 52–58.

(32) Bowne-Anderson, H.; Hibbel, A.; Howard, J. Regulation of Microtubule Growth and Catastrophe: Unifying Theory and Experiment. *Trends Cell Biol.* **2015,** *25,* 769–779.

(33) Desai, A.; Mitchison, T. J. Microtubule Polymerization Dynamics. *Annu. Rev. Cell Dev. Biol.* **1997**, *13,* 83–117.

(34) Nédélec, F.; Surrey, T.; Karsenti, E. Self-Organisation and Forces in the Microtubule Cytoskeleton. *Curr. Opin. Cell Biol.* **2003**, *15,* 118–124.

(35) Iglic, A.; Kulkarni, C. V. (Eds.) Advances in Planar Lipid Bilayers and Liposomes, Vol 19, **2014,** *19,* Elsevier Academic Press Inc, San Diego, CA USA.

(36) Tsuda, S.; Sakakura, T.; Fujii, S.; Suzuki, H.; Yomo, T. Shape Transformations of Lipid Vesicles by Insertion of Bulky-Head Lipids. *PLoS One* **2015,** *10,* e0132963.

(37) Czogalla, A.; Kauert, D. J.; Franquelim, H. G.; Uzunova, V.; Zhang, Y.; Seidel, R.; Schwille, P. Amphipathic DNA Origami Nanoparticles to Scaffold and Deform Lipid Membrane Vesicles. *Angew. Chemie-Int. Ed.* **2015,** *54,* 6501–6505.

(38) Brinkley, B. R. "Microtubule Organizing Centers". *Annual Reviews: Cell Biology* **1985**, *1,* 145–172.

(39) Tanaka-Takiguchi, Y.; Kakei, T.; Tanimura, A.; Takagi, A.; Honda, M.; Hotani, H.; Takiguchi, K. The Elongation and Contraction of Actin Bundles are Induced by Double-Headed Myosins in a Motor Concentration-Dependent Manner. *J. Mol. Biol.* **2004,** *341,* 467–476.

(40) Mirigian, M.; Mukherjee, K.; Bane, S. L.; Sackett, D. L. Measurement of *In Vitro* Microtubule Polymerization by Turbidity and Fluorescence. *Method Cell Biol.* **2013,** *115,* 215–229.

(41) Inaba, T.; Ishijima, A.; Honda, M.; Nomura, F.; Takiguchi, K.; Hotani, H. Formation and Maintenance of Tubular Membrane Projections Require Mechanical Force, but their Elongation and Shortening do not Require Additional Force. *J. Mol. Biol.* **2005**, *348*, 325–333.

(42) Kato, N.; Ishijima, A.; Inaba, T.; Nomura, F.; Takeda, S.; Takiguchi, K. Effects of Lipid Composition and Solution Conditions on the Mechanical Properties of Membrane Vesicles. *Membranes* **2015**, *5*, 22–47.

(43) Umeda, T.; Inaba, T.; Ishijima, A.; Takiguchi, K.; Hotani, H. Formation and Maintenance of Tubular Membrane Projections: Experiments and Numerical Calculations. *BioSystems* **2008,** *93,* 115–119.

(44) Carlier, M.-F.; Pantaloni, D. Kinetic Analysis of Guanosine 5'-Triphosphate Hydrolysis Associated with Tubulin Polymerization. *Biochemistry* **1981,** *20,* 1918–1924.

(45) O'Brien, T.; Voter, W. A.; Erickson, H. P. GTP Hydrolysis During Microtubule Assembly. *Biochemistry* **1987,** *26,* 4148–4156.

(46) Zou, Z.; Ding, Q.; Ou, L.; Yan, B. Efficient Production of Deoxynucleoside-5'-Monophosphates Using Deoxynucleoside Kinase Coupled with a GTP-Regeneration System. *Appl. Microbiol. Biotechnol.* **2013,** *97,* 9389–9395.

(47) Guevorkian, K.; Manzi, J.; Pontani, L.-L.; Brochard-Wyart, F.; Sykes, C. Mechanics of Biomimetic Liposomes Encapsulating an Actin Shell. *Biophys. J.* **2015,** *109,* 2471–2479.

(48) Summers, K.; Kirschner, M. W. Characteristics of the Polar Assembly and Disassembly of Microtubules Observed In Vitro by Dark Field Light Microscopy. *J. Cell Biol.* **1979,** *83,* 205–217.

(49) Minoura, I.; Hachikubo, Y.; Yamakita, Y.; Takazaki, H.; Ayukawa, R.; Uchimura, S.; Muto, E. Overexpression, Purification, and Functional Analysis of Recombinant Human Tubulin Dimer. *FEBS Lett.* **2013,** *587,* 3450–3455.

(50) Yamada, H.; Nagae, T.; Watanabe, N. High-Pressure Protein Crystallography of Hen Egg-White Lysozyme. *Acta. Cryst.* **2015,** *D71,* 742–753.

(51) Hamajima, Y.; Nagae, T.; Watanabe, N.; Ohmae, E.; Kato-Yamada, Y.; Kato, C. Pressure Adaptation of 3-Isopropylmalate Dehydrogenase from an Extremely Piezophilic Bacterium is Attributed to a Single Amino Acid Substitution. *Extremophiles* **2016,** *20,* 177–186.

(52) Fygenson, D. K.; Braun, E.; Libchaber, A. Phase Diagram of Microtubules. *Phys. Rev. E,* **1994,** *50,* 1579–1588.

(53) Mitchison, T.; Kirschner, M. Dynamic Instability of Microtubule Growth. *Nature*. **1984,** *312,* 237–242.

(54) Horio, T.; Hotani, H. Visualization of the Dynamic Instability of Individual Microtubules by Dark-Field Microscopy. *Nature* **1986,** *321,* 605–607.

(55) Fygenson, D. K.; Flyvbjerg, H.; Sneppen, K.; Libchaber, A.; Leibler, S. Spontaneous Nucleation of Microtubules. *Phys. Rev. E,* **1995,** *51,* 5059–5063.

(56) Gardner, M. K.; Charlebois, B. D.; Ja´nosi, I. M.; Howard, J.; Hunt, A. J.; Odde, D. J. Rapid Microtubule Self-Assembly Kinetics. *Cell* **2011,** *146,* 582–592.

(57) Permana, S.; Hisanaga, S.; Nagatomo, Y.; Iida, J.; Hotani, H.; Itoh. T. J. Truncation of the Projection Domain of MAP4 (Microtubule-Associated Protein 4) Leads to Attenuation of Microtubule Dynamics Instability. *Cell Struct. Funct.* **2005,** *29,* 147–158.

(58) Sixt, M.; Raz, E. (Eds.) Special Issue: Cell Adhesion and Migration. *Curr. Opin. Cell Biol.* **2015,** *36,* 1–122.

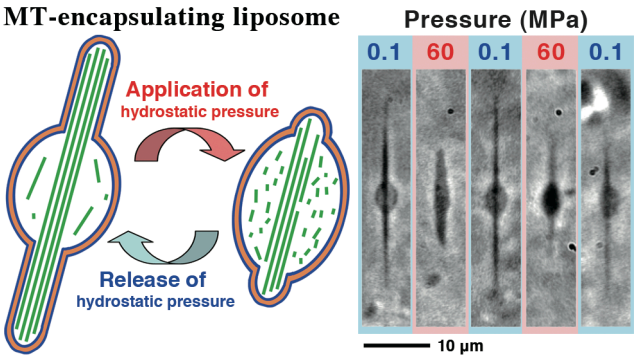

Table of Contents Graphic

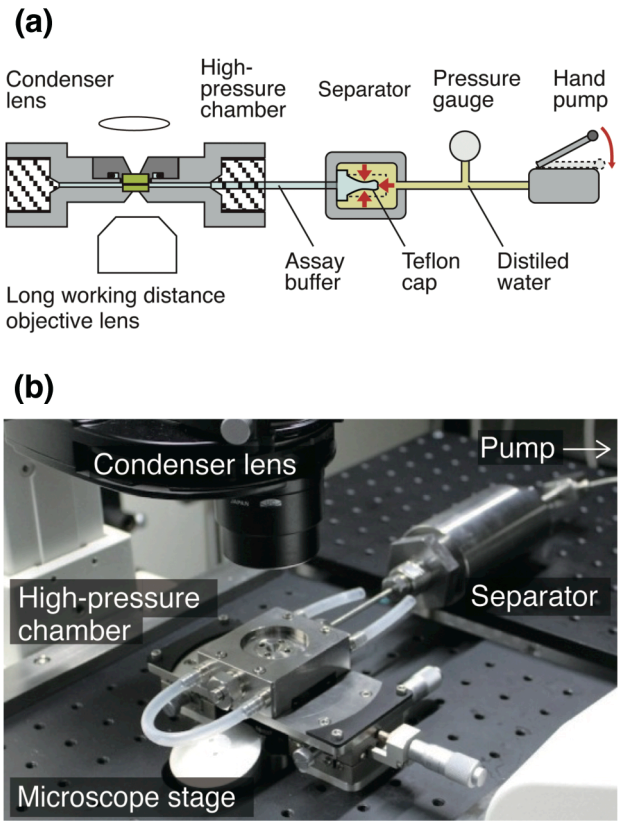

Figure 1. High-pressure microscope. **(a)** Schematic diagram of the high-pressure microscope. **(b)** Photograph of the high-pressure microscope.

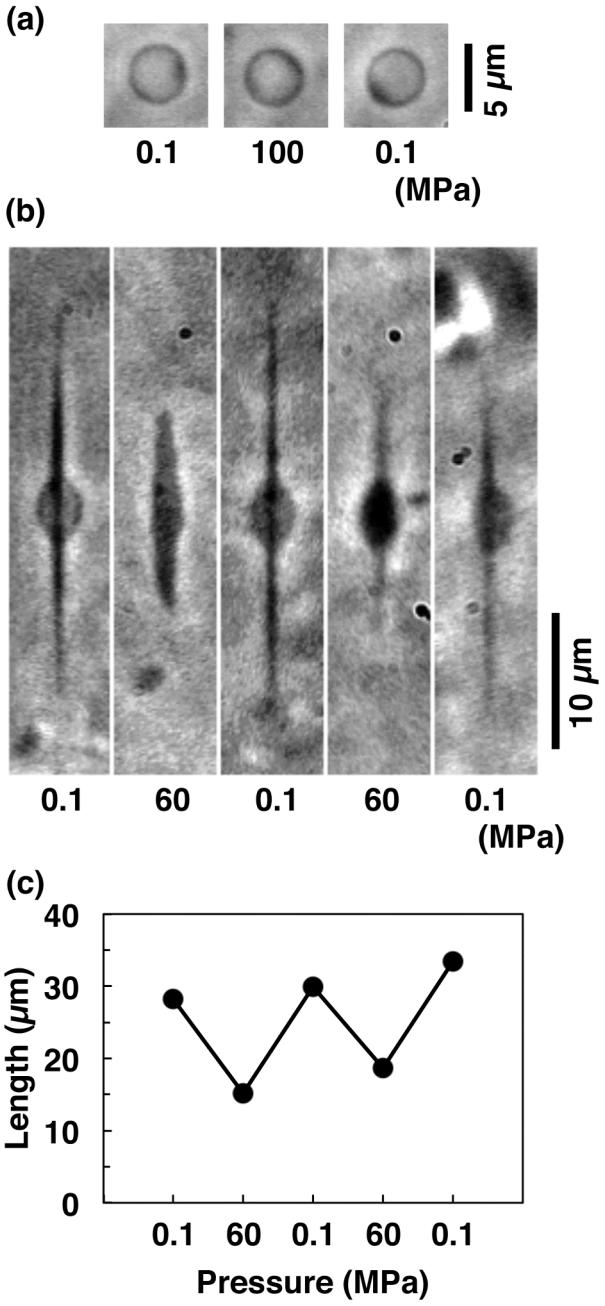

Figure 2. Reversible deformation of tubulin-encapsulating giant liposomes induced by the application and release of pressure. **(a)** Sequence of phase contrast images showing the morphology of a giant liposome that encapsulated no protein during changes in pressure (control). The liposome was spherical throughout the observation, and did not show any change in shape or size regardless of the pressure (Figure S1). **(b)** Sequence of phase contrast images showing the morphology of a giant liposome that encapsulated tubulin during changes in pressure. It is noted that the two images on the right side were average images of sequential video images within 5 sec in order to correct the defocus. In (a) and (b), the pressure applied is indicated at the bottom of each frame. Scale bars in (a) and (b) indicate 5 and 10 μm, respectively. It is noted here that, unless otherwise specified, each observed result shown in this report was obtained by tracking the morphological change of the same liposome. **(c)** End-to-end distance of the liposome in (b); shortening at 60 MPa occurred within 30 sec, and elongation at 0.1 MPa occurred within about 10 min (see Figure 3).

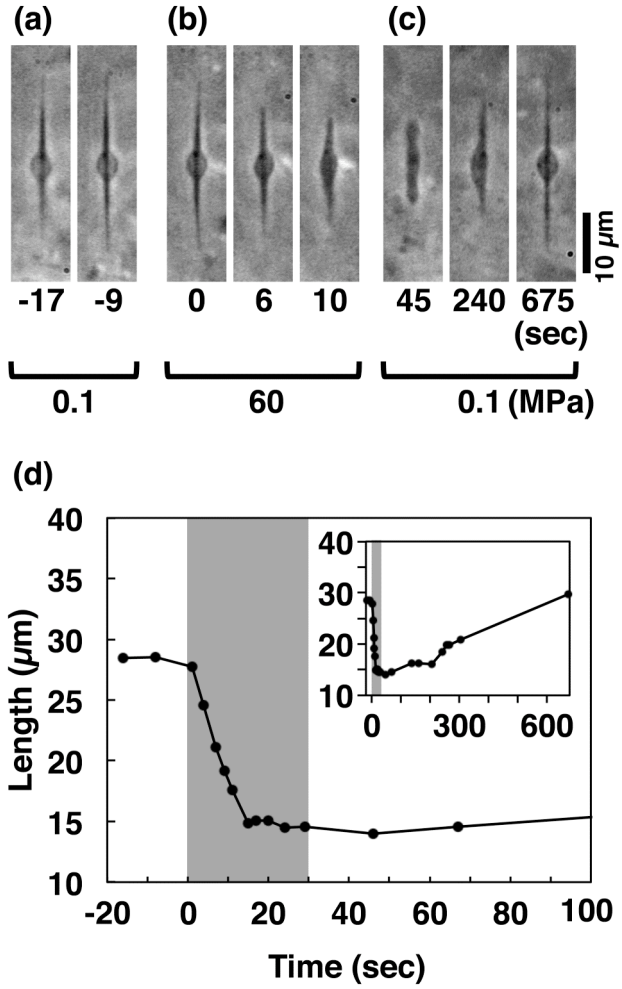

Figure 3. Reversible shrinkage of protrusions caused by the application and release of pressure. **(a, b,** and **c)** Sequence of phase contrast images of a MT-encapsulated giant liposome. The elapsed time (in sec) after the application of high pressure and the pressure (MPa) that has been applied are indicated at the bottom of each frame. At first, the hydrostatic pressure was 0.1 MPa (a), and the high pressure of 60 MPa was applied at the time of 0 sec (b). Then, at the time of 30 sec, the pressure was returned to 0.1 MPa (c). Scale bar indicates 10 μm. **(d)** Time course of the end-to-end distance between tips of protrusions of the liposome shown in (a − c). Inset shows the result of the whole period. The period when the pressure was 60 MPa is indicated by a gray background; at other periods, the pressure was 0.1 MPa. It should be noted that the shortening rate at 60 MPa was 0.92 μm/sec, and the elongation rate at 0.1 MPa was 2.5×10^{-2} μm/sec.

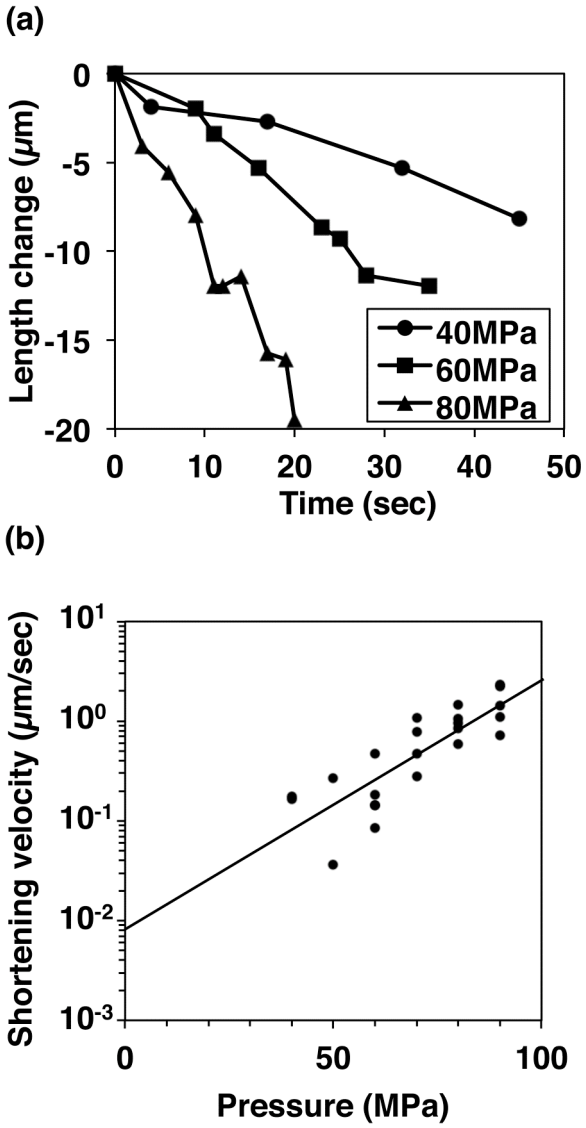

Figure 4. Shortening rate of the end-to-end distance between membrane protrusions of a liposome at high pressure. **(a)** Typical examples of the shortening process under various pressures. The cases of 40 (circles), 60 (squares) and 80 (triangles) MPa are shown. The high pressure was applied at the time of 0 sec. The results were obtained from different individual liposomes. **(b)** Semi-logarithmic plot of the shortening rate of the distance between the tips of the protrusions. The points plotted correspond to the results obtained from individual liposomes (n=21). The plots were fitted by Eq. 1 with $\alpha = 8.5 \times 10^{-3}$ μm/sec and $\Delta V^{\ddagger} = -0.23$ nm^3.

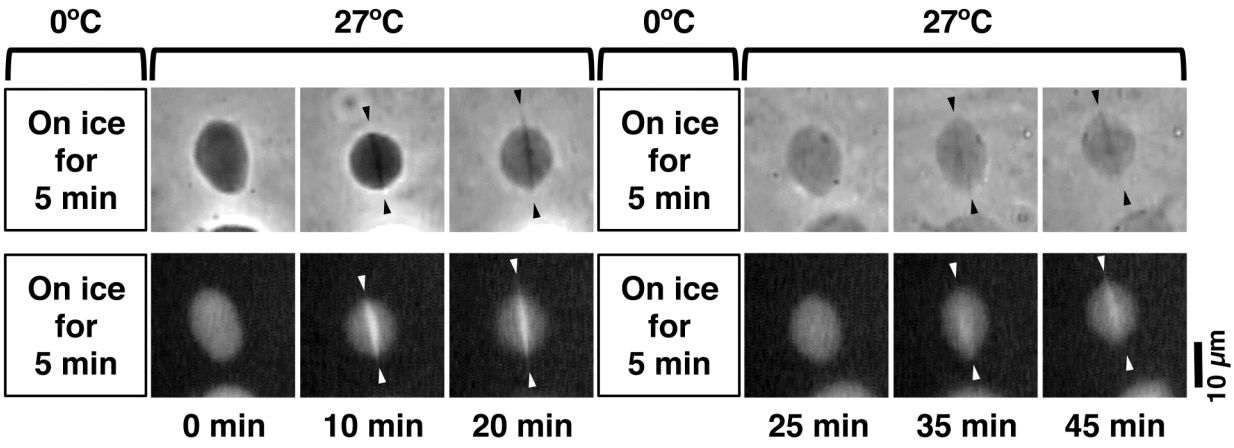

Figure 5. Reversible deformation of fluorescent-labeled tubulin-encapsulating liposomes controlled by temperature. Sequences of phase contrast (upper) and fluorescent (lower) images of a tubulin-encapsulated liposome are shown. The elapsed time (min) is indicated below each frame. The observation chamber was cooled on ice for 5 min just before t = 0 and 25 min, and was transferred to the microscope at 27°C. The scale bar indicates 10 μm. Positions of the tips of protrusions are indicated with arrowheads. The ratio of the fluorescence-labeled tubulin is 0.10 (mol/mol).

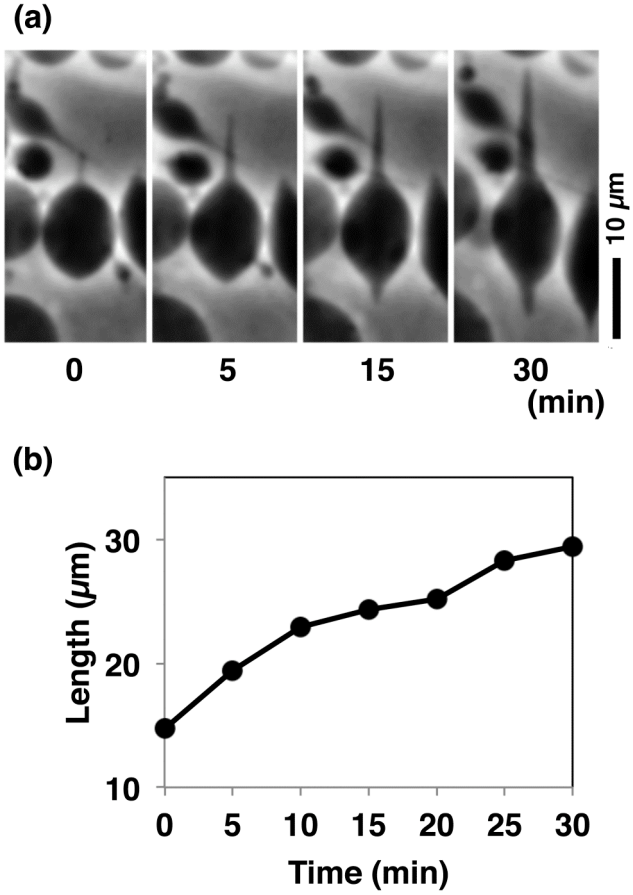

Figure 6. Reproduction of membrane protrusions of a MT-encapsulating giant liposome at 25°C after treatment on ice. **(a)** Sequence of phase contrast images of the liposome. The elapsed time (min) after the start of the observation is indicated at the bottom of each frame. The bar indicates 10 μm. **(b)** Time course of the end-to-end distance between the membrane protrusions of the liposome shown in (a).

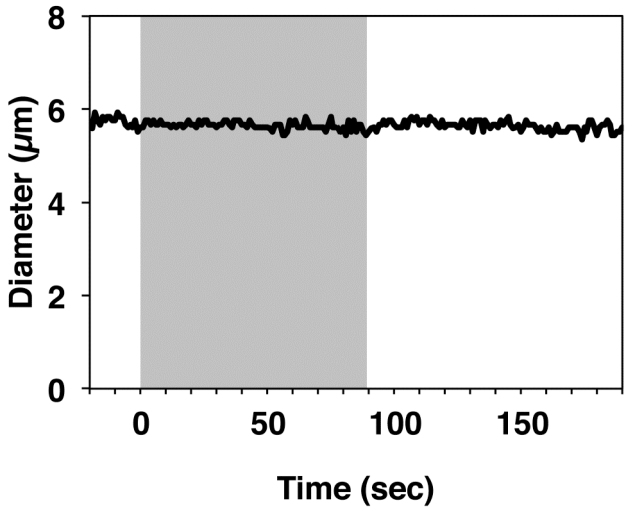

Figure S1. The diameter of a giant liposome that encapsulated no protein was plotted against the elapsed time after the start of the observation. The pressure applied was 0.1 MPa from −20 to 0 sec, 100 MPa from 0 to 90 sec, and 0.1 MPa from 90 to 190 sec. In the graph, the period when the pressure was 100 MPa is indicated by a gray background; at other periods, the pressure was 0.1 MPa.

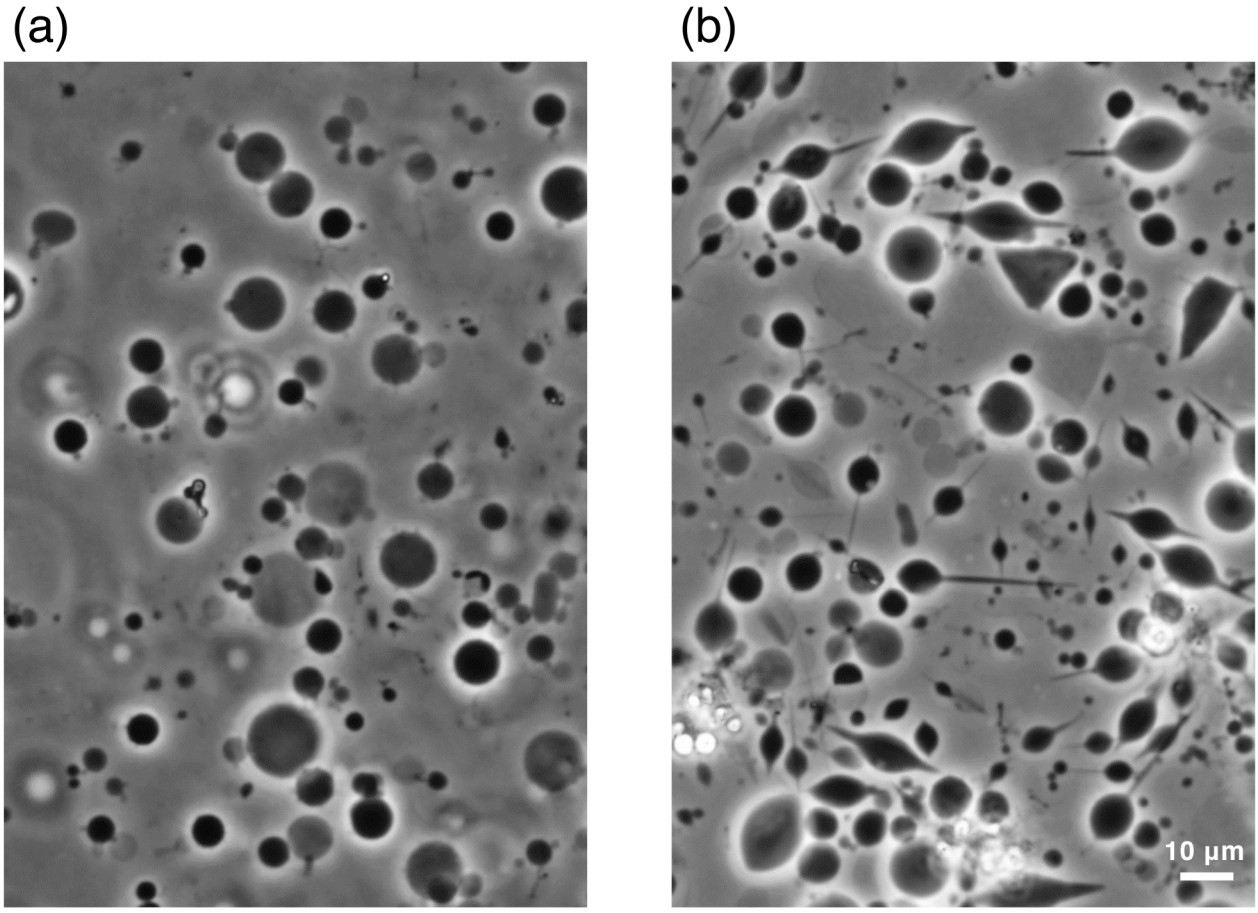

Figure S2. Regeneration of membrane protrusions of MT-encapsulating giant liposomes incubated on ice for 30 min **(a)** and then at 25°C for 2 hr **(b)**. In (a) and (b), different fields of the same specimen are shown, because fields where overlaps of the liposomes are small were selected to show their morphology clearly. The liposomes were prepared by the emulsion centrifugation method as described in Materials and Methods. The bar indicates 10 µm.

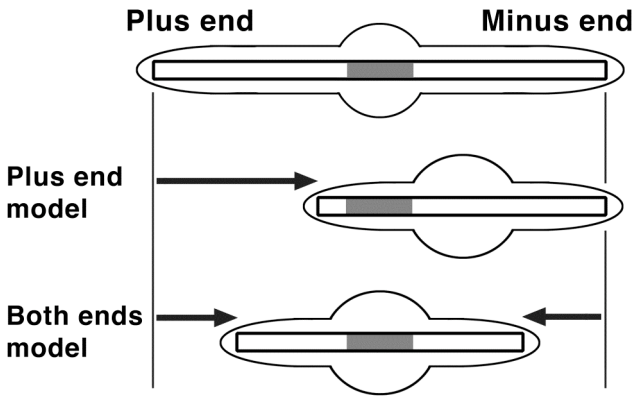

Figure S3. Model showing the relationship between the shortening of the end-to-end distance between the two membrane protrusions of a MT-encapsulating liposome (outer spindle-shaped frames) and the shortening of a MT that was encapsulated in the liposome (inner crossbars). For simplification, only one MT is drawn in each panel. In the upper panel, a MT-encapsulating liposome developing two protrusions at ambient pressure is shown. By application of hydrostatic pressure, the middle panel shows the case where MTs depolymerize only at the plus end, and the bottom panel shows the case where MTs depolymerize equally at both ends. Which shortening model is correct will be determined by experiments using a positioning marker fixed on the MTs, indicated as the grey region of the MT in each panel.

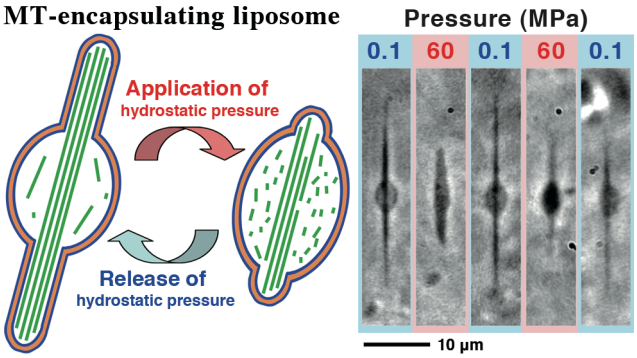

TOC

The effect of hydrostatic pressure on the morphology of tubulin-encapsulating cell-sized giant-liposomes is investigated using a high-pressure microscope. At ambient pressure, many liposomes formed protrusions similar to those produced by living cells, due to the assembly of MTs within the liposomes. The application of high pressure caused the protrusions to shrink. This process was reversible; after the pressure was released, the protrusions regenerated. This reversible deformation of liposomes was repeatedly inducible. The results demonstrate that regulating the assembling state of MTs inside liposomes by changing the hydrostatic pressure enables us to control the morphology of cell-sized liposomes repeatedly and reproducibly.